



# CHORUS

This is the accepted manuscript made available via CHORUS. The article has been published as:

## Physics-based statistical learning approach to mesoscopic model selection

Søren Taverniers, Terry S. Haut, Kipton Barros, Francis J. Alexander, and Turab Lookman

Phys. Rev. E **92**, 053301 — Published 9 November 2015

DOI: [10.1103/PhysRevE.92.053301](https://doi.org/10.1103/PhysRevE.92.053301)

# A physics-based statistical learning approach to mesoscopic model selection

Søren Taverniers,<sup>1</sup> Terry S. Haut,<sup>2</sup> Kipton Barros,<sup>3</sup> Francis J. Alexander,<sup>2</sup> and Turab Lookman<sup>3</sup>

<sup>1</sup>*Department of Mechanical and Aerospace Engineering,  
University of California, San Diego, 9500 Gilman Dr., La Jolla, CA 92093*

<sup>2</sup>*Computer, Computational, and Statistical Sciences Division,  
Los Alamos National Laboratory, Los Alamos, NM 87545*

<sup>3</sup>*Theoretical Division, Los Alamos National Laboratory, Los Alamos, NM 87545*

In materials science and many other research areas, models are frequently inferred without considering their generalization to unseen data. We apply statistical learning using cross-validation to obtain an optimally predictive coarse-grained description of a two-dimensional kinetic nearest-neighbor Ising model with Glauber dynamics ( $GD$ ) based on the stochastic Ginzburg-Landau equation ( $sGLE$ ). The latter is learned from  $GD$  “training” data using a log-likelihood analysis, and its predictive ability for various complexities of the model is tested on  $GD$  “test” data independent of the data used to train the model on. Using two different error metrics, we perform a detailed analysis of the error between magnetization time trajectories simulated using the learned  $sGLE$  coarse-grained description and those obtained using the  $GD$  model. We show that both for equilibrium and out-of-equilibrium  $GD$  training trajectories, the standard phenomenological description using a quartic free energy does not always yield the most predictive coarse-grained model. Moreover, increasing the amount of training data can shift the optimal model complexity to higher values. Our results are promising in that they pave the way for the use of statistical learning as a general tool for materials modeling and discovery.

PACS numbers: 05.10.-a, 02.70.-c, 05.20.-y, 05.45.Tp

Keywords: stochastic partial differential equations, Ginzburg-Landau equation, Ising model, statistical learning

## I. INTRODUCTION

Due to limitations in computational resources, the behavior of complex systems (e.g. climate, turbulent flow, materials under shock loading) often needs to be modeled using a coarse-grained description that captures the phenomenon of interest. Coarse-grained models cannot be perfect of course, since many microscopic degrees of freedom are absent. The Mori-Zwanzig formalism [1, 2] tells us that the relevant coarse-grained description should contain both noise [3, 4] and memory kernels to represent the “integrated out” fine scale dynamics. Deriving an appropriate coarse-graining analytically is therefore extremely difficult. Statistical learning provides a tractable way of finding a coarse-grained description that is able to predict the results of new experiments or simulations beyond those used in the model construction, which serves as a true objective test of the model. In fact, unlike traditional approaches, statistical learning can also serve as a coarse-graining strategy in cases where there is no clear separation of spatial and/or temporal scales. For example, it may be applied to problems that involve inhomogeneous flows (e.g. multi-component fluids, complex fluids) and those in materials science where the coarse-grained description needs to account for inhomogeneities at a finer scale, such as microstructural defects. Techniques such as the Heterogeneous Multiscale Method (HMM) [5] that demand a clean separation in time scales are not applicable.

In the statistical approach to coarse-graining discussed here, the goal is to search over a certain class of coarse-grained models and find the complexity for which the description is “optimally predictive”. This technique is called regularization, and to estimate the generalization error we use cross-validation. The latter involves randomly dividing data (either from experiments or simulations) into “training” and “test” samples. Ideally one would like both groups of data to be in-

finite, but in practice one only has a limited amount of data to work with. Experimentalists can only synthesize a small number of material samples, and in molecular dynamics simulations one is also limited to a finite number of samples. For the purposes of the current analysis, we will assume that the amount of training data is limited but that we can test our learned model on an infinite amount of data independent of the training samples. An extension to cases where both training *and* test data are finite will be the topic of future research.

Selecting the appropriate model regularization is of paramount importance because it can minimize both underfitting and overfitting. An underfitted model is too simplistic and therefore fails to capture much of the useful information available in the training data; hence, it will perform sub-optimally on data independent of the training set. In contrast, overfitting refers to the case where an overly complex model describes the many irrelevant details that appear in the training data by chance. An overfitted model will therefore be also less successful in generalizing to new data from simulations or experiments that are outside the class of the training data. The model developed in this study avoids common issues associated with overfitting by using an effectively infinite amount of test data independent of the samples on which it was trained, and selecting the complexity that makes it most predictive of this test data.

As an error estimator, cross-validation has been used for a number of years. When the amount of data is very limited though, there can be issues between the cross-validation error and the actual error [6, 7]. Moreover, a proper error analysis is often lacking in physics modeling applications. Our motivation is to learn mesoscale models from microstructural data incorporating prior domain knowledge and physical symmetries. We will focus on the time-dependent stochastic Ginzburg-Landau equation ( $sGLE$ ) which provides a coarse-grained description of a kinetic nearest-neighbor Ising model with Glauber dynamics ( $GD$ ) and of which the dynamics are

expected to be particularly straightforward to learn. While our approach is related to that in [8], we do not assume a prior distribution for the learned parameters and do not include a penalty for overfitting or complexity in the Bayesian Information Criterion. Moreover, instead of simply fitting a regular quartic free energy to a single or joint magnetization distribution function as in [9, 10], we consider higher order terms and find the parameters that optimally predict  $GD$  data independent of the samples on which the model was trained. The inclusion of terms beyond fourth order in the free energy accounts for the fact that we are in a regime of finite coarse-graining block sizes, and hence not at a fixed point in the renormalization group theory [11, 12]. Our current approach does not account for higher order spatial gradients, which can play an important role out of equilibrium; we plan to include these terms in future versions of the model. Finally, our study involves a detailed error analysis which is often lacking in existing literature on coarse-grained model selection.

Section II describes the microscopic  $GD$  model and its mesoscale description provided by the  $sGLE$ . Section III details our design loop used to select the optimal complexity of the  $sGLE$  for each amount of training data considered, after which Section IV discusses the results of the error analysis we performed in order to arrive at an optimally predictive model. Section V summarizes our conclusions and discusses possibilities for future work.

## II. THE KINETIC ISING MODEL AND ITS COARSE-SCALE DESCRIPTION BY A STOCHASTIC GINZBURG-LANDAU EQUATION

### A. Kinetic Ising model with Glauber dynamics

The Ising model with nearest-neighbor interactions [13] is a simple, yet very rich, model in statistical mechanics for describing ferromagnetic behavior. Consider a two-dimensional (2D) ferromagnet with atoms arranged on an  $N_1 \times N_2$  square lattice. The spin  $s_{i,j}$  (where  $i = 0, \dots, N_1 - 1$  and  $j = 0, \dots, N_2 - 1$ ) of each atom can be in one of two states,  $s_{i,j} = \pm 1$ , and can only interact with its four adjacent spins. We can add dynamics to this system by flipping spins with a certain transition rate  $w$ , and the result is a kinetic nearest-neighbor Ising model with spin-flip (Glauber) [14] dynamics (which we will refer to as  $GD$ ). This allows us to express the time evolution of the spin system through a master equation given by

$$\frac{d}{dt}\mathbb{P}(\sigma; t) = \sum_{\sigma'} [w(\sigma' \rightarrow \sigma)\mathbb{P}(\sigma'; t) - w(\sigma \rightarrow \sigma')\mathbb{P}(\sigma; t)] \quad (1)$$

where  $\mathbb{P}(\sigma; t)$  is the joint probability of finding the system in spin configuration  $\sigma$  at time  $t$ , and the  $w$ 's are the transition rates between two  $N_1 \times N_2$ -spin configurations differing only in the value of 1 spin,  $s_{i,j}$ . For  $w$  we choose the heat bath rate, given by

$$w_{HB}(\sigma \rightarrow \sigma') = \kappa \left( 1 + e^{-\beta[\mathcal{H}(\sigma) - \mathcal{H}(\sigma')] } \right)^{-1}. \quad (2)$$

Here  $\mathcal{H}(\sigma)$  represents the Hamiltonian of the spin system with configuration  $\sigma$ ,  $\beta = 1/(k_B T)$  with  $T$  the system temperature, and  $\kappa^{-1}$  sets the time scale of the spin-flip process and can depend both on  $T$  and the spins other than  $s_{i,j}$ . We simulate this kinetic Ising model via a Monte Carlo (MC) algorithm with 1 MC step per spin; i.e., to complete one step in our Ising run, we perform  $N_1 \times N_2$  times the following procedure:

1. Pick a random site  $(i, j)$  where  $i = 0, \dots, N_1 - 1$  and  $j = 0, \dots, N_2 - 1$ .
2. Draw a number  $r_1$  from a uniform distribution on  $[0, 1]$ .
3. Flip the spin  $s_{i,j}$  if  $r_1 < w(\sigma \rightarrow \sigma')$ , or leave it in its original state if  $r_1 \geq w(\sigma \rightarrow \sigma')$ .

In all of our work here, we initialize the lattice by selecting spins to be +1 or -1 randomly based on drawing samples from a discrete uniform distribution on the interval  $[-1, 0) \cup (0, 1]$ .

### B. Ginzburg-Landau equation

By invoking a phenomenological coarse-graining approach, it is possible to obtain a mesoscopic model of  $GD$  given by a time-dependent Ginzburg-Landau equation ( $GLE$ ) [15]. The latter will describe the spatio-temporal evolution of an ‘‘order parameter’’,  $\phi$ , a field variable which represents the instantaneous average of Ising spin values over some portion of a ferromagnetic material (also called ‘‘magnetization’’). At finite temperatures, one needs to account for fluctuations, which can be added via a white noise term to obtain an overdamped stochastic relaxation equation

$$\frac{\partial \phi(x, t)}{\partial t} = -M \frac{\delta F[\phi(x, t)]}{\delta \phi(x, t)} + \eta(x, t), \quad (3)$$

with  $M$  the mobility which sets the time scale of the dynamics. Here  $\eta(x, t)$  is a zero-mean Gaussian white noise with a variance which, according to the fluctuation-dissipation theorem, scales linearly with  $M$  and the system temperature. Moreover,  $F[\phi]$  is an effective free energy for the system, and is usually developed as a power series in  $\phi$  and its derivatives

$$F \sim \sum_k a_k \phi^k + b \nabla^2 \phi + c \nabla^4 \phi + d \phi \nabla^2 \phi + \dots \quad (4)$$

In the context of late-stage domain growth, renormalization group arguments indicate that the Ising model with Glauber dynamics is in the universality class of Model A dynamics [12], and hence well represented at the coarse scale by having only  $a_2$  and  $a_4$  different from zero. However, since we are focusing on intermediate time and length scales, we relax this assumption and instead consider a model class for the free energy consisting of even-term polynomials with degree two or greater. The complexity that we eventually select is the one for which the model is optimally predictive of  $GD$  data independent of the samples from which it was learned.

### III. NUMERICAL ALGORITHM

Our goal is to learn the parameters of a discrete version of the stochastic Ginzburg-Landau equation (*sGLE*) which evolves the magnetization  $\phi$  from time  $t_n$  to time  $t_{n+1}$  according to

$$\begin{aligned} \phi_{i,j,n+1} = & \phi_{n,i,j} + \alpha_0(\phi_{n,i+1,j} + \phi_{n,i-1,j} + \phi_{n,i,j+1} \\ & + \phi_{n,i,j-1} - 4\phi_{n,i,j}) + \sum_{k=0}^{\frac{C-1}{2}} \alpha_{k+1} \phi_{n,i,j}^{2k+1} \\ & + \alpha_{(C+3)/2} \xi_{n,i,j}, \end{aligned} \quad (5)$$

where  $C$  is the model complexity [16] and the  $\xi_{n,i,j}$  are independent, identically distributed standard normal random variables. Here  $n$  and  $n+1$  refer to times  $t_n$  and  $t_{n+1}$ ,  $i = 0, \dots, \bar{N}_1 - 1$  and  $j = 0, \dots, \bar{N}_2 - 1$ , with  $\bar{N}_1$  and  $\bar{N}_2$  the number of coarse-grained Ising spin blocks in both spatial directions. Given block-averaged training data  $S_{n,i,j}$ , we would like to find the set of parameters  $\alpha_{opt} \equiv \alpha_0, \alpha_1, \dots, \alpha_{(C+3)/2}$  that maximizes the likelihood of observing  $S_0, S_1, \dots, S_{n_{eq}-1}$  [17] using the *sGLE* model. It turns out  $\alpha_{opt}$  is the solution to a linear system

$$A\alpha_{opt} = \mathbf{b}, \quad (6)$$

where the components of  $A$  and the elements of  $\mathbf{b}$  involve products of  $S_n$ , its powers and its discrete Laplacian. The dimension of this system is given by the number of free parameters that make up the model (5), which is equal to  $(C-1)/2 + 3$ . For more details, we refer the reader to Appendix A where we have worked out the case of  $C = 3$ . We then test our learned *sGLE* model against independent *GD* data (“test” data) to ascertain how well learned models of different complexities perform on unseen data. By calculating the root-mean-square (RMS) error between *GD* test trajectories and those simulated using the learned *sGLE*, we then determine for which complexity  $C$  the latter is optimally predictive of the *GD* test data.

We will consider two error metrics in our analysis, which we will refer to as “type 1” and “type 2” error. For type 1 error, we calculate the *sGLE* grid at time  $t_{n+1}$  through (5) but replace  $\phi_n$  with the block-averaged *GD* test data at time  $t_n$ . This error is of the same type as the error that we want to minimize when calculating  $\alpha_{opt}$  from the *GD* training data, where we search for the set of parameters that maximizes the likelihood of observing the training data at  $t_{n+1}$  given the *sGLE* model and the training data at  $t_n$ , for every  $n$  (see Appendix A). For type 2 error, we evolve the *sGLE* grid in time through (5) directly, i.e. we do not keep referring back to the *GD* test data at each time  $t_n$ .

A flowchart of the operational algorithm is shown in Figure 1. At a high level, our approach for computing one data point in the error probability density function (pdf) for a learned *sGLE* model of complexity  $C$ , given a number of training samples  $N_{train}$ , can be described as follows (see Appendix B for more details).

1. We simulate  $N_{test}$  independent *GD* test sample trajectories. For each trajectory, we let the Ising system

evolve over  $n_{mc}$  steps, after which we take another  $n_{eq}$  steps during which we record the Ising configuration. Each of these steps represents one MC step per spin as detailed in Section II A.

2. We simulate  $N_{train}$  independent *GD* training sample trajectories. We let the spins evolve over  $n_{mc}$  steps, and then record their configuration over the next  $n_{eq}$  steps.
3. Using the data gathered during the last  $n_{eq}$  steps of each training trajectory, we compute the coefficients of the learned *sGLE* polynomial using a log-likelihood analysis (see Appendix A).
4. With the parameters calculated in step 3, we now simulate  $N_{test}$  *sGLE* trajectories. Each trajectory consists of  $n_{eq}$  steps, with each step involving the advancement of the discrete *sGLE* (5) from one discrete point in time to the next.
5. For the  $k$ th *sGLE* trajectory, we calculate the RMS error  $\varepsilon_k$  between this trajectory and the  $k$ th block-averaged *GD* test trajectory.
6. Finally, we compute the test-averaged error

$$\varepsilon = \frac{1}{N_{test}} \sum_{k=1}^{N_{test}} \varepsilon_k, \quad (7)$$

which we will call “type 1” or “type 2” test error depending on how the *sGLE* trajectory has been calculated (see our above definition of these errors).

The quantity  $\varepsilon$  represents one point in the error pdf for the considered complexity  $C$  and number of training samples  $N_{train}$ . The entire pdf is then obtained by repeating the above procedure except for step 1 (we use the same *GD* test trajectories for each point in the pdf)  $n_{real}$  number of times. **We will denote the sample (i.e., realization) mean and variance of this pdf by  $\bar{\varepsilon}$  and  $s_\varepsilon^2$ , respectively.**

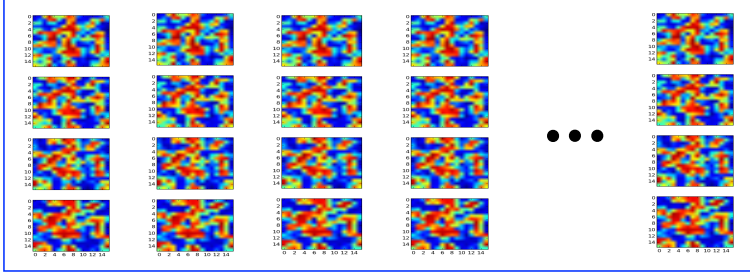
### IV. ERROR ANALYSIS AND MAIN RESULTS

We now present the pdfs of type 1 and type 2 error, defined in Section III, for different complexities  $C = 3, 5, 7$  or  $9$ , given a finite number of *GD* training samples  $N_{train}$ . We will use  $N_{test} = 1000$  *GD* test samples, which provides an accurate generalization error [18]. Moreover, we will build up the error histograms using  $n_{real} = 5000$  independent realizations, and consider both training data in equilibrium and out of equilibrium. For the equilibrium case, we measure the energy of the spin system and choose  $n_{mc}$  as the number of steps after which thermal equilibrium has been reached. Out of equilibrium, we choose  $n_{mc}$  such that after  $n_{mc}$  steps domains have started to form. Learning the *sGLE* model parameters from *GD* data for which the block size is smaller than the size of a typical domain allows the Laplacian in the *sGLE* to better capture gradients in the *GD* data, and should hence yield a more accurate coarse-grained description. For both cases, we determine an appropriate value for  $n_{eq}$  through trial and error,

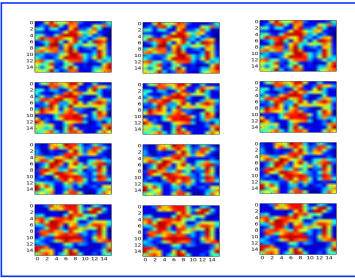
Step 1: Pick *sGLE* model complexity  $C$

$$\phi_{i,j,n+1} = \phi_{n,i,j} + \alpha_0(\phi_{n,i+1,j} + \phi_{n,i-1,j} + \phi_{n,i,j+1} + \phi_{n,i,j-1} - 4\phi_{n,i,j}) + \sum_{k=0}^{\frac{C-1}{2}} \alpha_{k+1} \phi_{n,i,j}^{2k+1} + \alpha_{(C+3)/2} \xi_{n,i,j}$$

Step 2: Generate  $N_{test}$  independent Ising test samples



Step 3: Generate  $N_{train} \ll N_{test}$  independent Ising training samples



Step 4: Learn *sGLE* model parameters through log-likelihood analysis

$$\underset{\alpha}{\operatorname{argmax}} \ln \mathbb{P}(S_0, S_1, \dots, S_{n_{eq}-1}; \alpha) \rightarrow \alpha_{opt}$$

Step 5: Generate  $N_{test}$  *sGLE* model samples using  $\alpha_{opt}$  and compare with Ising test samples

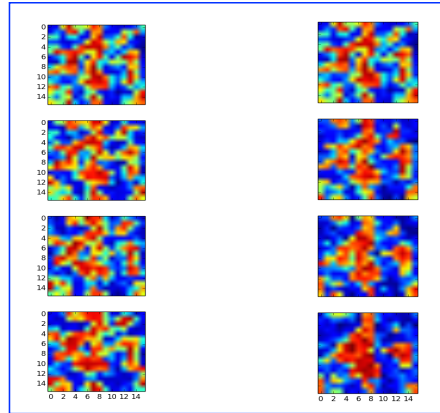


Figure 1. (Color online) Flowchart for the model complexity selection algorithm.

and choose values that provide a sufficient amount of input data to our log-likelihood solver. We will use  $n_{mc} = 2000$  and  $n_{eq} = 100$  for the equilibrium case, and  $n_{mc} = n_{eq} = 500$  out of equilibrium. In all cases, we simulate the Glauber dynamics on a  $256 \times 256$  spin lattice with periodic boundary conditions, and coarse grain using  $16 \times 16$  blocks. Finally, next to each error distribution, we show a plot of the free energy constructed using the learned model parameters. These plots are meant to serve as a check of the physical soundness of our approach in the sense that, consistent with common knowledge, a single-well potential should be observed above the phase transition and a double-well potential below the phase transition. However, they do not convey any information regarding the predictiveness of our model, which follows entirely from the error distributions.

### A. Type 1 test error pdfs for training data in equilibrium

We first consider the case where we train on  $N_{train} = 8$   $GD$  trajectories in equilibrium, obtained by quenching the spin lattice from infinite temperature to either  $T = 1.6 J/k_B$  (below  $T_c = 2.269 J/k_B$  [19]) or  $T = 2.8 J/k_B$  (above  $T_c$ ), letting the system evolve over  $n_{mc} = 2000$  steps and then sampling over  $n_{eq} = 100$  steps. As Figure 2 shows, at  $T = 1.6 J/k_B$  the error pdf's sample mean  $\bar{\epsilon}$  clearly decreases with complexity  $C$ . Hence, the most predictive  $sGLE$  model is that with the highest complexity considered,  $C = 9$ .

At  $T = 2.8 J/k_B$ , however, the error pdfs for all the complexities overlap almost completely (see Figure 3), indicating that the regular third-order  $sGLE$  polynomial is adequate to predict the coarse-grained Glauber dynamics.

### B. Type 1 test error pdfs for training data out of equilibrium

Next, we look at the case where we train on various amounts of  $GD$  trajectories out of equilibrium, obtained by quenching the spin lattice from infinite temperature to  $T = 2.2 J/k_B$  (just below  $T_c$ ), evolving it over  $n_{mc} = 500$  steps and then sampling over  $n_{eq} = 500$  steps.

As Figures 4 through 7 show, regardless of the amount of training data the regular  $\phi^4$  form of the free energy ( $C = 3$ ) is not optimally predictive of the  $GD$  test data. The complexity for which the  $sGLE$  model best predicts the  $GD$  test trajectories varies with the amount of training data. For small amounts of training data (i.e.  $N_{train} = 1$  or  $2$ ), the histograms for the different complexities largely overlap. As the number of training samples is increased to 16, the pdfs for  $C = 5$  and higher can be more clearly distinguished from that for  $C = 3$ . When one further increases the amount of training samples to 128, the pdf for  $C = 3$  becomes fully distinct from those for higher complexities, and the pdf for  $C = 5$  is becoming more distinct from those for  $C = 7$  and  $C = 9$ . In sum, increasing the amount of  $GD$  training data causes the complexity at which the  $sGLE$  is optimally predictive to shift toward higher values.

### C. Type 2 test error pdfs for training data out of equilibrium

Finally, we repeat the simulations in Section IV B for type 2 error. We find that for this error type the regular  $\phi^4$  free energy *does* optimally predict the  $GD$  test data, regardless of the amount of training data. Figure 8 shows this for the case of 1  $GD$  training sample. We note here that it is to be expected that  $\bar{\epsilon}$  is bigger for type 2 error than for type 1 error, since the latter is calculated in the same way as the optimization error for obtaining the  $\alpha_{opt}$  is calculated from the  $GD$  training data, while the former is not.

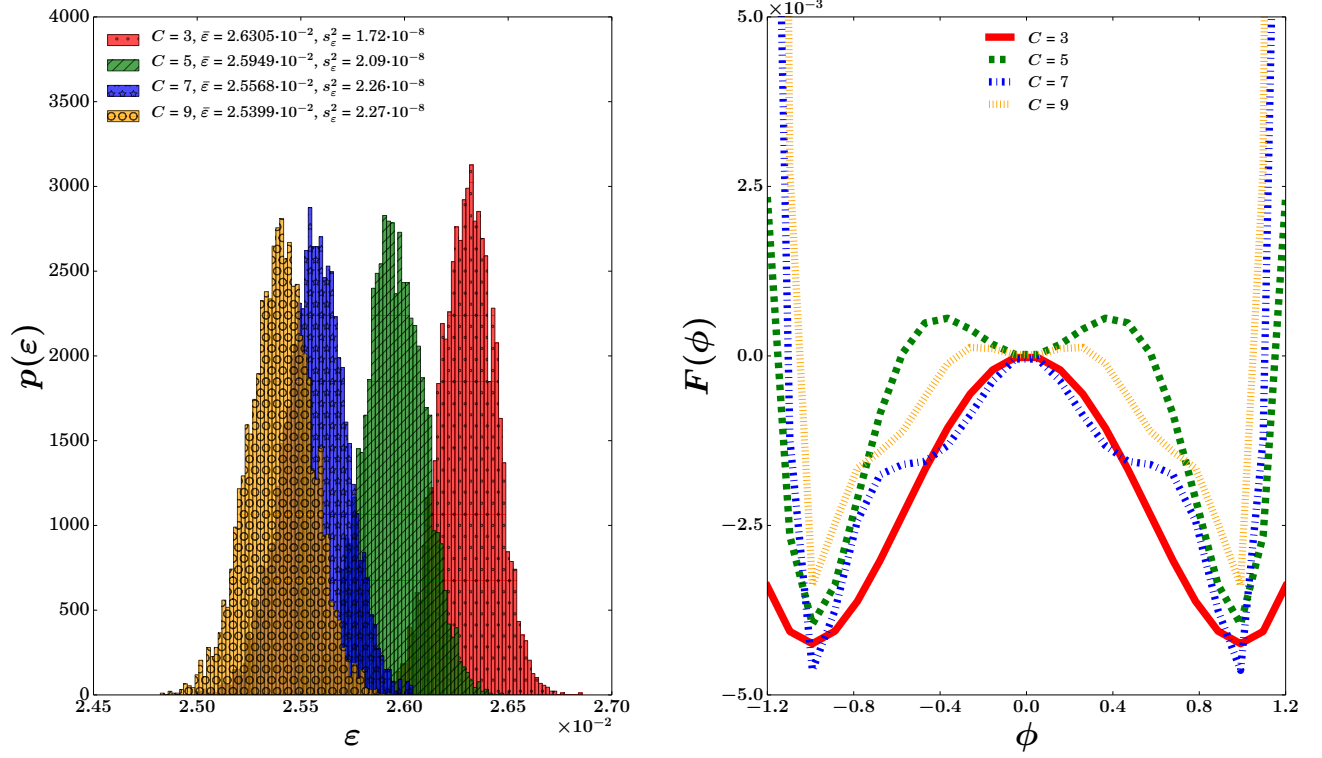


Figure 2. (Color online) Type 1 error pdfs (left) and learned Ginzburg-Landau free energy (right) for different complexities of an *sGLE* model learned from 8 equilibrium *GD* training samples at  $T = 1.6 J/k_B$  (below the phase transition). The *sGLE* with  $C = 9$  predicts the *GD* test data best.

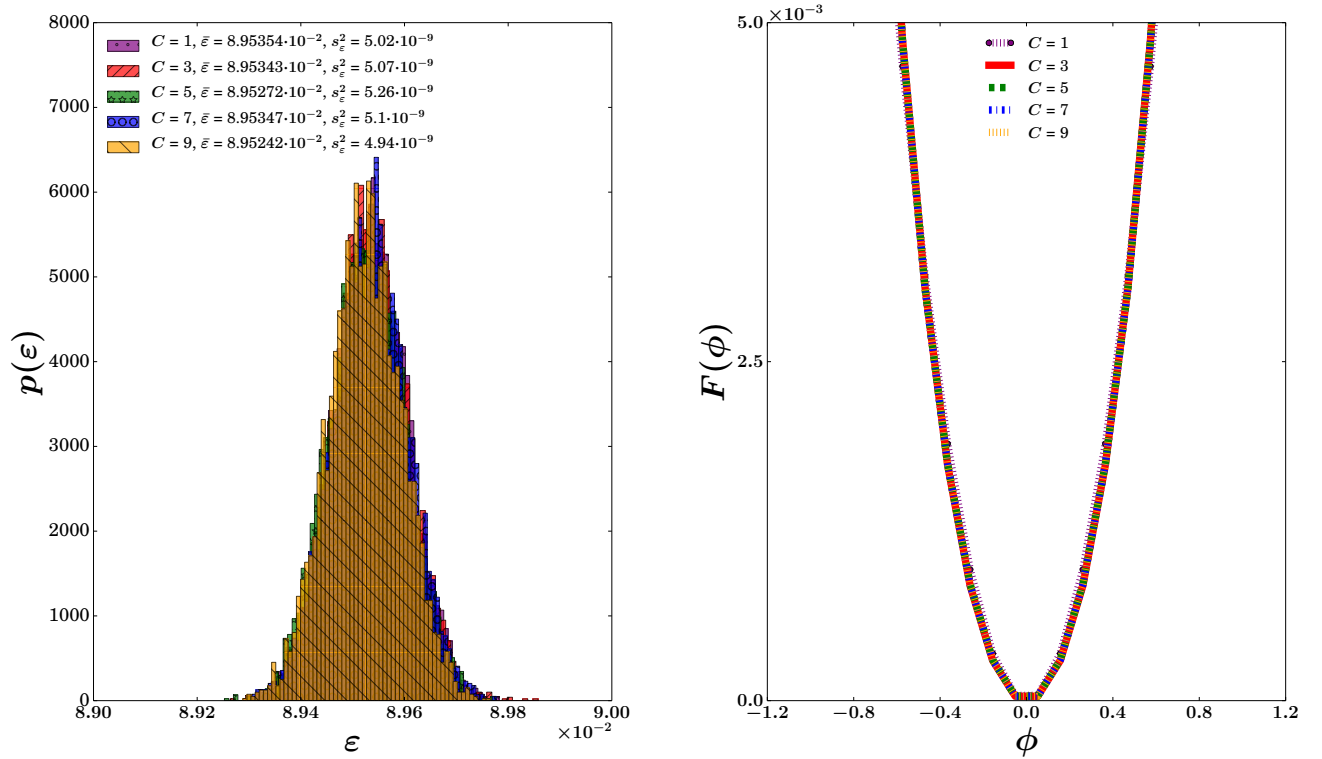


Figure 3. (Color online) Type 1 error pdfs for different complexities of an *sGLE* model learned from 8 equilibrium *GD* training samples at  $T = 2.8 J/k_B$  (above the phase transition). All considered model complexities are equally predictive of the *GD* test data.

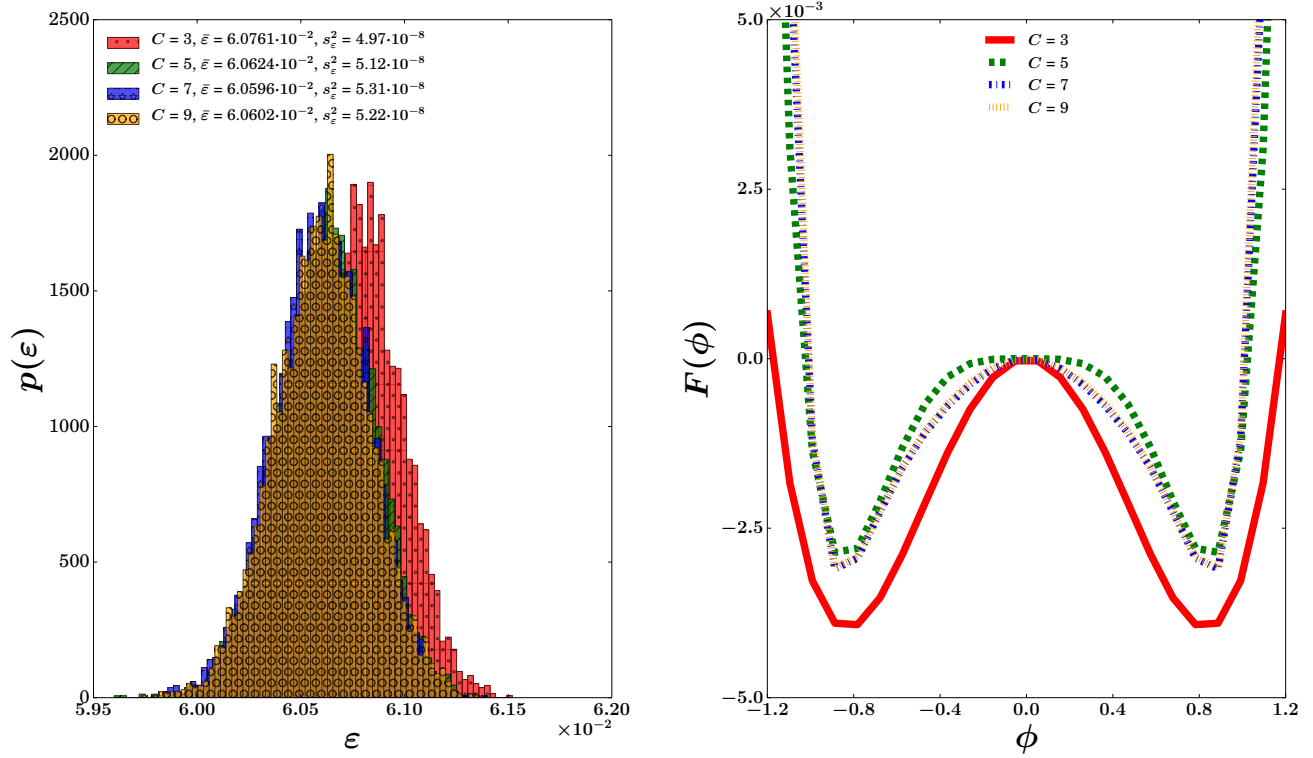


Figure 4. (Color online) Type 1 error pdfs for different complexities of an  $sGLE$  model learned from 1 out-of-equilibrium  $GD$  training sample at  $T = 2.2 J/k_B$  (just below the phase transition). Complexities 5 and higher are optimally predictive of the  $GD$  test data, but the corresponding error pdfs still largely overlap with that for  $C = 3$ .

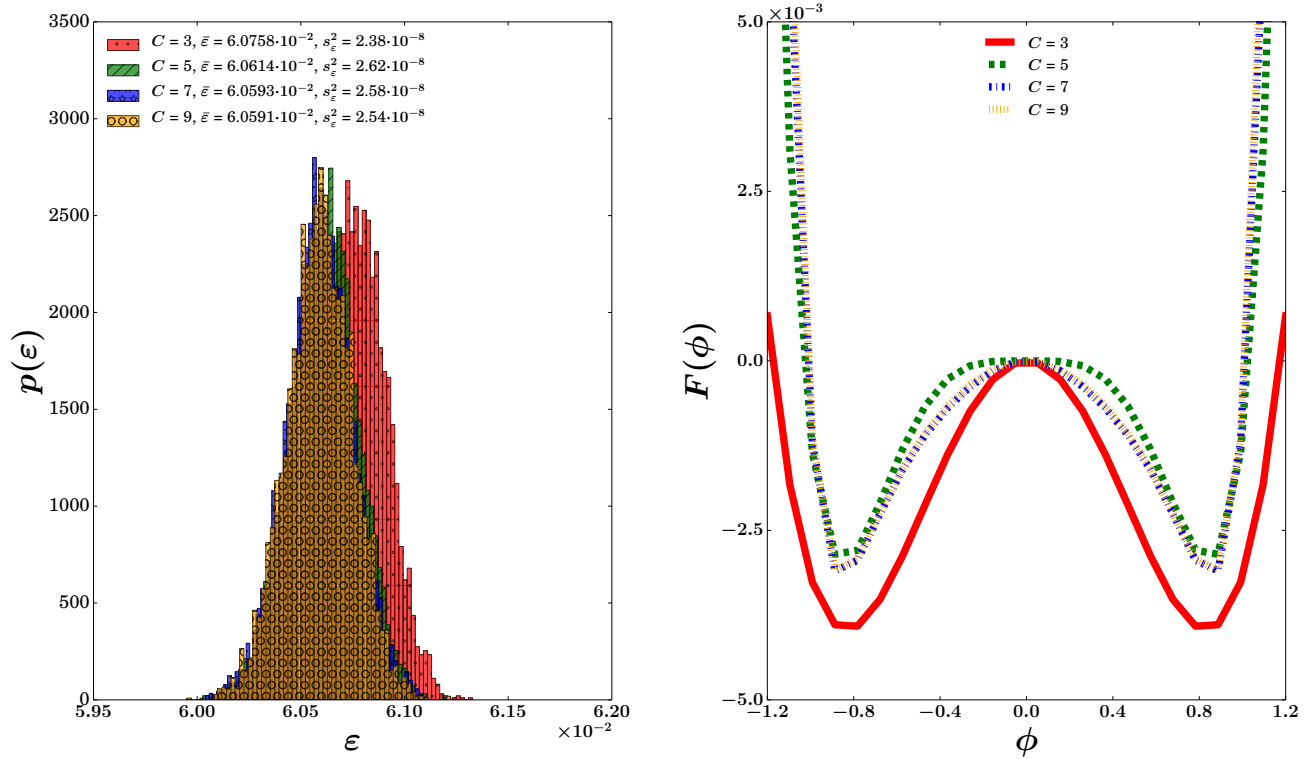


Figure 5. (Color online) Type 1 error pdfs for different complexities of an  $sGLE$  model learned from 2 out-of-equilibrium  $GD$  training samples at  $T = 2.2 J/k_B$ .

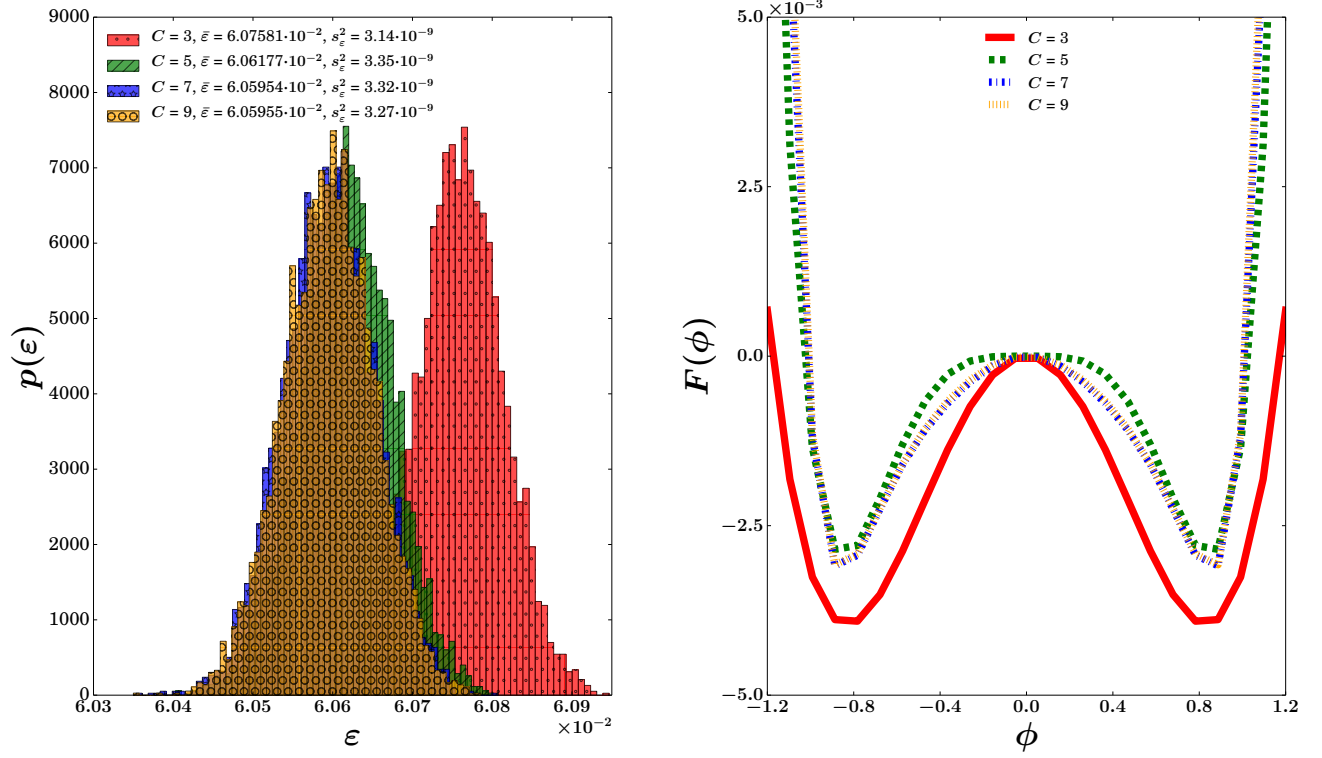


Figure 6. (Color online) Type 1 error pdfs for different complexities of an *sGLE* model learned from 16 out-of-equilibrium *GD* training samples at  $T = 2.2 J/k_B$ . The error pdfs for  $C = 5$  and higher are now clearly distinct from that for  $C = 3$ .

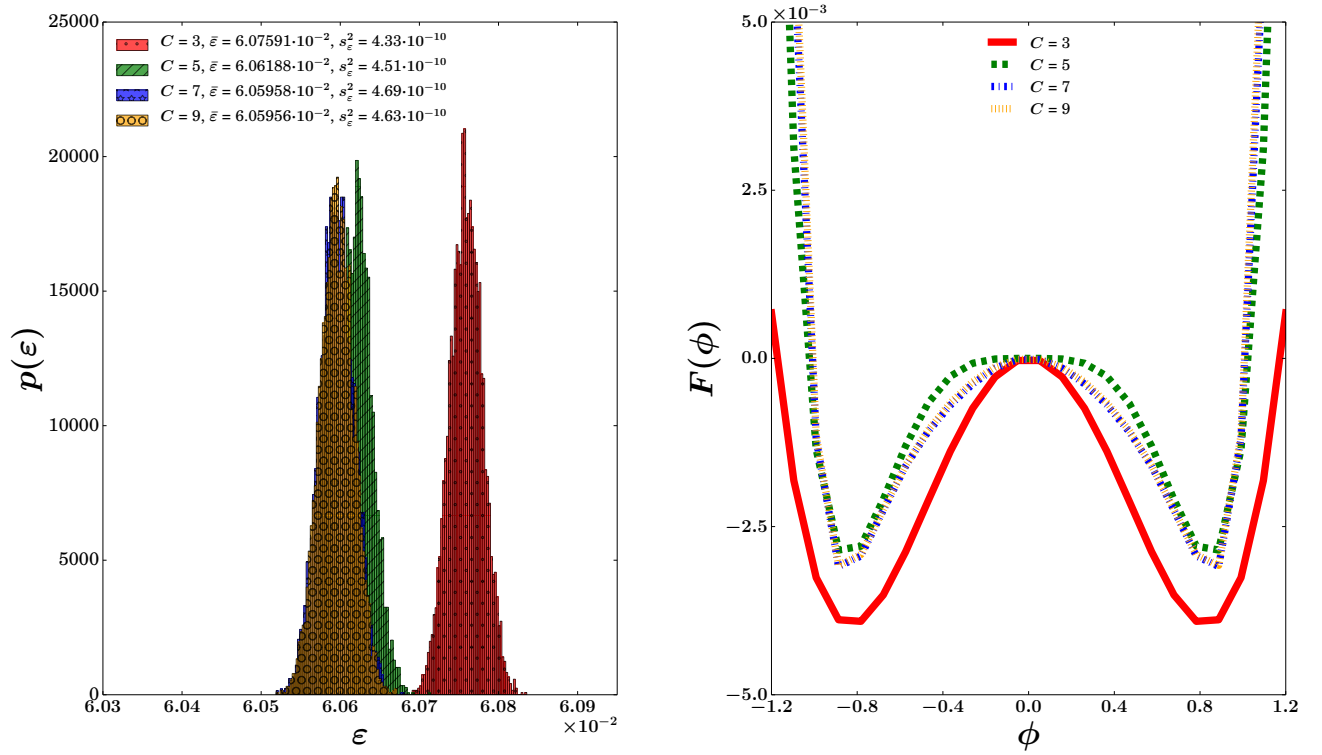


Figure 7. (Color online) Type 1 error pdfs for different complexities of an *sGLE* model learned from 128 out-of-equilibrium *GD* training samples at  $T = 2.2 J/k_B$ . The error pdf for  $C = 5$  and those for  $C = 7$  and higher are becoming more distinct, shifting the optimally predictive model complexity to  $C = 7$ .

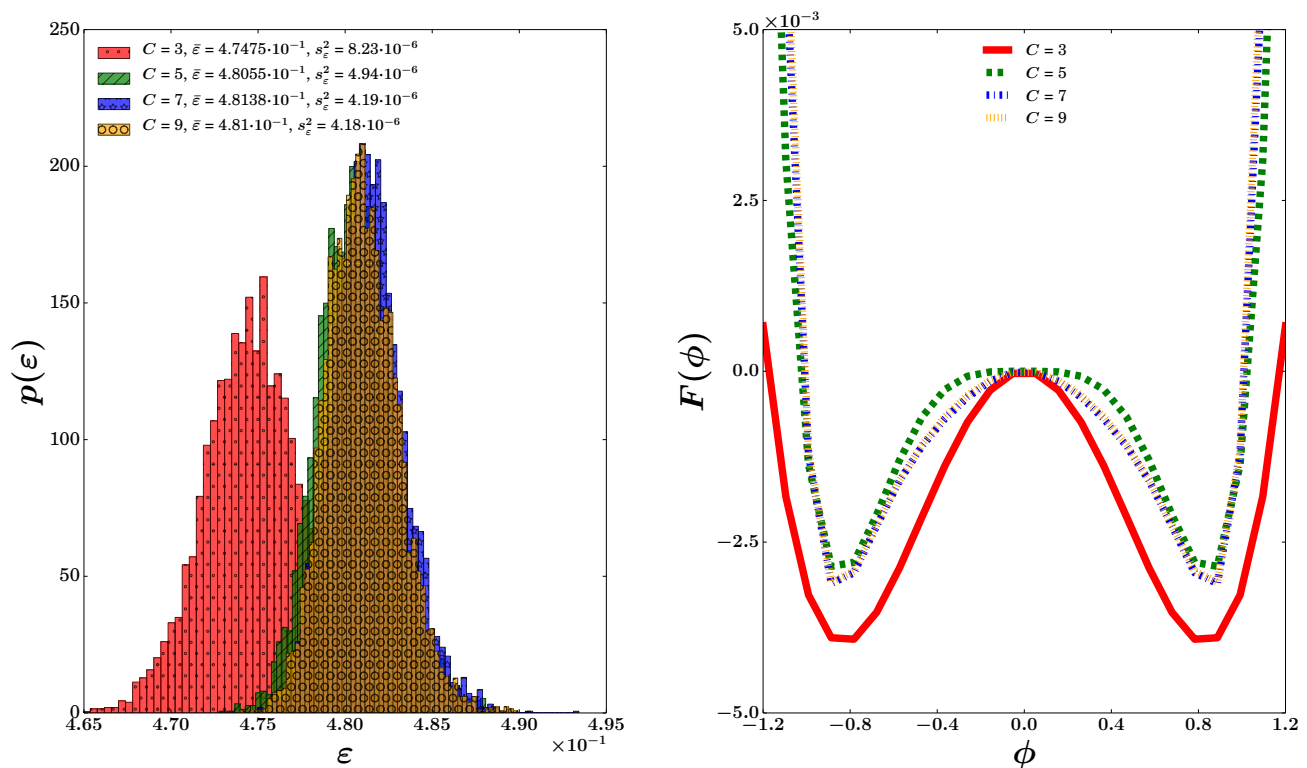


Figure 8. (Color online) Type 2 error pdfs for different complexities of an  $sGLE$  model learned from 1 out-of-equilibrium  $GD$  training sample at  $T = 2.2 J/k_B$ . The  $sGLE$  with  $C = 3$  is most predictive of the  $GD$  test data.

## V. SUMMARY AND CONCLUSIONS

By performing a detailed error analysis in the context of a statistical learning approach using cross-validation, we derive an optimally predictive coarse-grained description of a two-dimensional kinetic nearest-neighbor Ising model with Glauber dynamics ( $GD$ ) based on the stochastic Ginzburg-Landau equation ( $sGLE$ ). The latter is learned from microscopic  $GD$  “training” data through a log-likelihood analysis, and its capacity to predict  $GD$  “test” data independent of the training data is analyzed for various model complexities using two error metrics and varying amounts of training data.

Our analysis yields the following major conclusions:

1. For type 1 error, a complexity of 3 in the  $sGLE$  force equation does *not* yield an optimally predictive model for any amount of training data that we investigated. Moreover, the model complexity yielding the most predictive coarse-grained description increases with the amount of  $GD$  training data.
2. For type 2 error, the regular Ginzburg-Landau description using a  $\phi^4$  mean-field free energy *does* yield the most predictive model irrespective of the amount of  $GD$  training data.

The principled methodology developed here for simple Model A dynamics can be applied to more complicated problems such as Model H dynamics [12]. A particular application which might benefit from this work is the use of data

generated from experiments, e.g. ultrafast X-ray diffraction patterns of structural phase transitions in semiconductor crystals to generate models describing crystal disordering [20]. In general, our approach can be utilized in any application using a Ginzburg-Landau functional, e.g. in phase field simulations of materials.

Directions for future work include studying the effects of the coarse-graining block size (in both space and time), performing a rigorous analysis of the stability and discretization error of our numerical scheme, and expanding the model class by including operator terms that account for higher order spatial gradients. Moreover, it is desirable to complement the current computational analysis with a rigorous theoretical derivation of an expression for the error probability density function in terms of model complexity, number of training samples and coarse-graining block size.

## VI. ACKNOWLEDGMENTS

This work was carried out under the auspices of the Department of Energy at Los Alamos National Laboratory under Contract LA-UR-15-23538. The authors are grateful for support from the LANL LDRD-DR project #20140013DR. They would also like to thank Avadh Saxena for helpful discussions.

### Appendix A: Computation of the parameters in the learned $sGLE$ model

In order to calculate the coefficients of the learned discrete  $sGLE$ , we employ the widely used statistical technique of maximizing the log-likelihood that the model will predict the  $GD$  training data. The discrete  $sGLE$  we are trying to learn has the form

$$\begin{aligned} \phi_{n+1,i,j} &= \phi_{n,i,j} + \alpha_0(\phi_{n,i+1,j} + \phi_{n,i-1,j} + \phi_{n,i,j+1} \\ &\quad + \phi_{n,i,j-1} - 4\phi_{n,i,j}) + \sum_{k=0}^{\frac{C-1}{2}} \alpha_{k+1} \phi_{n,i,j}^{2k+1} \\ &\quad + \alpha_{(C+3)/2} \xi_{n,i,j}, \end{aligned} \quad (\text{A1})$$

where  $C$  is the model complexity (we only consider odd complexities), the  $\xi_{n,i,j}$  are independent, identically distributed standard normal random variables and  $n = 0, \dots, n_{eq}-2$ ,  $i = 0, \dots, \bar{N}_1 - 1$  and  $j = 0, \dots, \bar{N}_2 - 1$ . Given the block-averaged training data  $S_{n,i,j}$ , we would like to find the set of parameters  $\alpha_{opt} \equiv \alpha_0, \alpha_1, \dots, \alpha_{(C+3)/2}$  that maximizes the probability of observing  $S_0, S_1, \dots, S_{n_{eq}-1}$  from model (A1). The latter is given by

$$\begin{aligned} \mathbb{P}(S_0, S_1, \dots, S_{n_{eq}-1}; \alpha) \\ &= \mathbb{P}(S_0) \mathbb{P}(S_1 | S_0; \alpha) \dots \mathbb{P}(S_{n_{eq}-1} | S_1, \dots, S_{n_{eq}-2}; \alpha) \\ &= \mathbb{P}(S_0) \mathbb{P}(S_1 | S_0; \alpha) \dots \mathbb{P}(S_{n_{eq}-1} | S_{n_{eq}-2}; \alpha). \end{aligned} \quad (\text{A2})$$

Given  $S_n$ , we can see from (A1) that for each  $i$  and  $j$ ,  $S_{n+1,i,j}$  is normally distributed with mean

$$\begin{aligned} Y_{n,i,j} &= S_{n,i,j} + \alpha_0(S_{n,i+1,j} + S_{n,i-1,j} + S_{n,i,j+1} \\ &\quad + S_{n,i,j-1} - 4S_{n,i,j}) + \sum_{k=0}^{\frac{C-1}{2}} \alpha_{k+1} S_{n,i,j}^{2k+1} \end{aligned} \quad (\text{A3})$$

and variance  $\alpha_{(C+3)/2}^2$ . Therefore, we have

$$\begin{aligned} \mathbb{P}(S_{n+1,i,j} = s | S_n; \alpha) \\ &= \frac{1}{\alpha_{(C+3)/2} \sqrt{2\pi}} \exp \left[ -\frac{(s - Y_{n,i,j})^2}{2\alpha_{(C+3)/2}^2} \right], \end{aligned} \quad (\text{A4})$$

and since the  $\xi_{n,i,j}$  are independent,

$$\begin{aligned} \mathbb{P}(S_{n+1} | S_n; \alpha) \\ &= \frac{1}{(\alpha_{(C+3)/2}^2 2\pi)^{(\bar{N}_1 \bar{N}_2)/2}} \exp \left[ -\frac{\|S_{n+1} - Y_n\|^2}{2\alpha_{(C+3)/2}^2} \right]. \end{aligned} \quad (\text{A5})$$

Hence,

$$\begin{aligned} \ln \mathbb{P}(S_0, S_1, \dots, S_{n_{eq}-1}; \alpha) \\ &= - \sum_{n=0}^{n_{eq}-2} \frac{\|S_{n+1} - Y_n\|^2}{2\alpha_{(C+3)/2}^2} \\ &\quad - (n_{eq} - 1) \bar{N}_1 \bar{N}_2 \ln(\alpha_{(C+3)/2}) + \text{constant}. \end{aligned} \quad (\text{A6})$$

For notational simplicity, let us now focus on the case of  $C = 3$ ; the generalization to higher order nonlinearity is straightforward. From (A6), it follows that we need to minimize

$$\begin{aligned} \mathcal{L}(S_1, \dots, S_{n_{eq}-1}; \alpha) &= \frac{1}{2} \alpha_3^{-2} f(\alpha_0, \alpha_1, \alpha_2) \\ &\quad + (n_{eq} - 1) \bar{N}_1 \bar{N}_2 \ln(\alpha_3), \end{aligned} \quad (\text{A7})$$

where

$$\begin{aligned} f(\alpha_0, \alpha_1, \alpha_2) &= \sum_{n=0}^{n_{eq}-2} \sum_{i=0}^{\bar{N}_1-1} \sum_{j=0}^{\bar{N}_2-1} [(S_{n+1,i,j} - S_{n,i,j}) \\ &\quad - \alpha_0(S_{n,i+1,j} + S_{n,i-1,j} + S_{n,i,j+1} \\ &\quad + S_{n,i,j-1} - 4S_{n,i,j}) - \alpha_1 S_{n,i,j} \\ &\quad - \alpha_2 S_{n,i,j}^3]^2. \end{aligned} \quad (\text{A8})$$

From

$$\frac{\partial \mathcal{L}}{\partial \alpha_3} = -\alpha_3^{-3} f(\alpha_0, \alpha_1, \alpha_2) + (n_{eq} - 1) \bar{N}_1 \bar{N}_2 \alpha_3^{-1} = 0, \quad (\text{A9})$$

we can solve for  $\alpha_3$

$$\alpha_3 = \sqrt{\frac{f(\alpha_0, \alpha_1, \alpha_2)}{(n_{eq} - 1) \bar{N}_1 \bar{N}_2}}. \quad (\text{A10})$$

Also, for  $k \neq 3$ , we have

$$\frac{\partial \mathcal{L}}{\partial \alpha_k} = \frac{1}{2} \alpha_3^{-2} \frac{\partial f}{\partial \alpha_k}. \quad (\text{A11})$$

If we now define

$$\begin{aligned} D_{n,i,j} &= S_{n+1,i,j} - S_{n,i,j}, \\ A_{n,i,j} &= S_{n,i+1,j} + S_{n,i-1,j} + S_{n,i,j+1} + S_{n,i,j-1} - 4S_{n,i,j}, \\ B_{n,i,j} &= S_{n,i,j}, \quad C_{n,i,j} = S_{n,i,j}^3, \end{aligned} \quad (\text{A12})$$

then

$$\begin{aligned} \frac{\partial f}{\partial \alpha_0} &= \partial_{\alpha_0} \sum_{n=0}^{n_{eq}-2} \sum_{i=0}^{\bar{N}_1-1} \sum_{j=0}^{\bar{N}_2-1} (D_{n,i,j} - \alpha_0 A_{n,i,j} \\ &\quad - \alpha_1 B_{n,i,j} - \alpha_2 C_{n,i,j})^2 \\ &= -2 \left( \sum_{n=0}^{n_{eq}-2} \sum_{i=0}^{\bar{N}_1-1} \sum_{j=0}^{\bar{N}_2-1} D_{n,i,j} A_{n,i,j} \right) \\ &\quad + 2 \left( \sum_{n=0}^{n_{eq}-2} \sum_{i=0}^{\bar{N}_1-1} \sum_{j=0}^{\bar{N}_2-1} A_{n,i,j}^2 \right) \alpha_0 \\ &\quad + 2 \left( \sum_{n=0}^{n_{eq}-2} \sum_{i=0}^{\bar{N}_1-1} \sum_{j=0}^{\bar{N}_2-1} B_{n,i,j} A_{n,i,j} \right) \alpha_1 \\ &\quad + 2 \left( \sum_{n=0}^{n_{eq}-2} \sum_{i=0}^{\bar{N}_1-1} \sum_{j=0}^{\bar{N}_2-1} C_{n,i,j} A_{n,i,j} \right) \alpha_2 \\ &= -2(a_0 - a_{00}\alpha_0 - a_{01}\alpha_1 - a_{02}\alpha_2). \end{aligned} \quad (\text{A13})$$

Similarly,

$$\frac{\partial f}{\partial \alpha_1} = -2(a_1 - a_{10}\alpha_0 - a_{11}\alpha_1 - a_{12}\alpha_2), \quad (\text{A14})$$

where

$$\begin{aligned} a_1 &= \sum_{n=0}^{n_{eq}-2} \sum_{i=0}^{\bar{N}_1-1} \sum_{j=0}^{\bar{N}_2-1} D_{n,i,j} B_{n,i,j}, \\ a_{10} &= \sum_{n=0}^{n_{eq}-2} \sum_{i=0}^{\bar{N}_1-1} \sum_{j=0}^{\bar{N}_2-1} A_{n,i,j} B_{n,i,j}, \\ a_{11} &= \sum_{n=0}^{n_{eq}-2} \sum_{i=0}^{\bar{N}_1-1} \sum_{j=0}^{\bar{N}_2-1} B_{n,i,j}^2, \\ a_{12} &= \sum_{n=0}^{n_{eq}-2} \sum_{i=0}^{\bar{N}_1-1} \sum_{j=0}^{\bar{N}_2-1} C_{n,i,j} B_{n,i,j}. \end{aligned} \quad (\text{A15})$$

Finally,

$$\frac{\partial f}{\partial \alpha_2} = -2(a_2 - a_{20}\alpha_0 - a_{21}\alpha_1 - a_{22}\alpha_2), \quad (\text{A16})$$

where

$$\begin{aligned} a_2 &= \sum_{n=0}^{n_{eq}-2} \sum_{i=0}^{\bar{N}_1-1} \sum_{j=0}^{\bar{N}_2-1} D_{n,i,j} C_{n,i,j}, \\ a_{20} &= \sum_{n=0}^{n_{eq}-2} \sum_{i=0}^{\bar{N}_1-1} \sum_{j=0}^{\bar{N}_2-1} A_{n,i,j} C_{n,i,j}, \\ a_{21} &= \sum_{n=0}^{n_{eq}-2} \sum_{i=0}^{\bar{N}_1-1} \sum_{j=0}^{\bar{N}_2-1} B_{n,i,j} C_{n,i,j}, \\ a_{22} &= \sum_{n=0}^{n_{eq}-2} \sum_{i=0}^{\bar{N}_1-1} \sum_{j=0}^{\bar{N}_2-1} C_{n,i,j}^2. \end{aligned} \quad (\text{A17})$$

Hence, we need to solve the linear system

$$\begin{aligned} a_{00}\alpha_0 + a_{01}\alpha_1 + a_{02}\alpha_2 &= a_0, \\ a_{10}\alpha_0 + a_{11}\alpha_1 + a_{12}\alpha_2 &= a_1, \\ a_{20}\alpha_0 + a_{21}\alpha_1 + a_{22}\alpha_2 &= a_2. \end{aligned} \quad (\text{A18})$$

We can see that despite the nonlinearity of the  $sGLE$ , optimizing the log-likelihood function can be reduced to solving a linear system.

## Appendix B: Details of the operational procedure for calculating the error pdfs

To compute one data point in the error pdf for a learned  $sGLE$  model of complexity  $C$  given a number of training samples  $N_{train}$ , we do the following.

1. We simulate  $N_{test}$  independent  $GD$  test sample trajectories. The  $k$ th trajectory is obtained as follows:

- (a) Starting from a random initial Ising configuration, we march over  $n_{mc} - 1$  steps.
- (b) Starting from the resulting Ising configuration, we march over  $n_{eq} - 1$  steps and store the block-averaged time history over these steps in a 3D matrix  $s^{av,test}$  with dimensions  $n_{eq} \times \bar{N}_1 \times \bar{N}_2$ . Here  $\bar{N}_1$  and  $\bar{N}_2$  represent the number of spin blocks in each spatial direction.
- (c) This matrix  $s^{av,test}$  will be the  $k$ th element of a 4D matrix  $s^{av,test,all}$  with dimensions  $N_{test} \times n_{eq} \times \bar{N}_1 \times \bar{N}_2$ .

The initial spins  $s_{i,j}$  ( $i = 0, \dots, \bar{N}_1 - 1$  and  $j = 0, \dots, \bar{N}_2 - 1$ ) are given by  $s_{i,j} = 1 - 2r_{i,j}$ , where the  $r_{i,j}$  are drawn from a discrete uniform distribution on the half-open interval  $[0, 2)$ . Furthermore, with ‘‘block-averaged time history’’, we refer to the time evolution of the block-averaged spin configuration of the Ising lattice. At each discrete point in time, we group the individual spins into blocks of a certain size, and then calculate the average spin values over the different blocks. The resulting coarsened grid is then recorded.

2. We simulate  $N_{train}$  independent  $GD$  training sample trajectories. A trajectory is calculated as follows:

- (a) Starting from a random initial Ising configuration, we march over  $n_{mc} - 1$  steps.
- (b) Starting from the final Ising configuration, we march over  $n_{eq} - 1$  steps and store the block-averaged time history over these steps in a 3D matrix  $s^{av,train}$  with dimensions  $n_{eq} \times \bar{N}_1 \times \bar{N}_2$ .
- (c) We concatenate  $s^{av,train}$  of the current training sample with the corresponding matrices of the previous training samples along the first (time) dimension, and hence obtain a bigger matrix  $s^{av,train,all}$  with dimensions  $N_{train} \times n_{eq} \times \bar{N}_1 \times \bar{N}_2$ .

3. Using the training data stored in  $s^{av,train,all}$ , we compute the coefficients of the learned  $sGLE$  polynomial using a log-likelihood analysis (see Appendix A).

4. With the parameters calculated in step 3, we now simulate  $N_{test}$   $sGLE$  trajectories. The  $k$ th trajectory is obtained as follows:

- (a) We define a 3D matrix  $\phi$  with dimensions  $n_{eq} \times \bar{N}_1 \times \bar{N}_2$ .
- (b) We take the block-averaged Ising test configuration stored in  $s_{k,0,::}$  as the initial condition and define  $s^{av,test} \equiv s_{k,::}$ . We then define  $\phi_{0,::} \equiv s_{0,::}$ .
- (c) We march over  $n_{eq} - 1$  steps and store the time history over these steps in  $\phi$ .
- (d) The configuration  $\phi_{n+1,::}$  is calculated according to

$$\phi_{n+1,i,j} = x_{i,j} + \mathcal{G}(x_{:,i}; \alpha), \quad (\text{B1})$$

where  $x_{:,j}$  is either  $s_{n,::}^{av,test}$  or  $\phi_{n,::}$ ,  $i = 0, \dots, \bar{N}_1 - 1$  and  $j = 0, \dots, \bar{N}_2 - 1$ .

In (d), we have defined  $\mathcal{G}(x_{:,j}; \alpha)$  as

$$\begin{aligned} \mathcal{G}(x_{:,j}; \alpha) &= \alpha_0(x_{i+1,j} + x_{i-1,j} + x_{i,j+1} + x_{i,j-1} - 4x_{i,j}) \\ &\quad + \sum_{k=0}^{\frac{C-1}{2}} \alpha_{k+1}(x_{i,j})^{2k+1} + \alpha_{(C+3)/2} \xi_{n,i,j}. \end{aligned} \quad (\text{B2})$$

5. For the  $k$ th  $sGLE$  trajectory, we calculate the RMS er-

ror  $\varepsilon_k$

$$\varepsilon_k = \sqrt{\frac{1}{a} \sum_{n=0}^{n_{eq}-2} \sum_{i=0}^{\bar{N}_1-1} \sum_{j=0}^{\bar{N}_2-1} (\phi_{n+1,i,j} - s_{n+1,i,j}^{av,test})^2}, \quad (\text{B3})$$

where  $a = (n_{eq} - 1)\bar{N}_1\bar{N}_2$ .

6. Finally, we compute the test-averaged error

$$\varepsilon = \frac{1}{N_{test}} \sum_{k=1}^{N_{test}} \varepsilon_k, \quad (\text{B4})$$

which we will call “type 1” test error if the  $\phi_{n+1,i,j}$  are calculated using  $x_{:,j} = s_{n,::}^{av,test}$  in (B1), or “type 2” test error if the  $\phi_{n+1,i,j}$  are calculated using  $x_{:,j} = \phi_{n,::}$  in (B1).

- 
- [1] H. Mori, Progress of Theoretical Physics **33**, 3 (1965).  
[2] R. Zwanzig, J. Stat. Phys. **9**, 3 (1973).  
[3] J. B. Bell, J. Foo, and A. L. Garcia, J. Comput. Phys. **223**, 1 (2007).  
[4] S. Taverniers, F. J. Alexander, and D. M. Tartakovsky, J. Comput. Phys. **262** (2014).  
[5] E. Weinan, B. Engquist, X. Li, and V.-E. E. Ren, W., Journal Communications in Computational Physics **2**, 3 (2007).  
[6] L. A. Dalton and E. R. Dougherty, Pattern Recognition **45**, 6 (2012).  
[7] L. A. Dalton and E. R. Dougherty, Pattern Recognition **46**, 5 (2013).  
[8] B. C. Daniels and I. Nemenman, ArXiv, Submitted (2014).  
[9] K. Kaski, K. Binder, and J. D. Gunton, J. Phys. A: Math. Gen., **16** (1983).  
[10] K. Kaski, K. Binder, and J. D. Gunton, Phys. Rev. B **29**, 3996 (1984).  
[11] A. J. Bray, Advances in Physics **43**, 3 (1994).  
[12] P. C. Hohenberg and B. I. Halperin, Rev. Mod. Phys. **49**, 3 (1977).  
[13] E. Ising, Z. Phys., **31** (1925).  
[14] R. J. Glauber, J. Math. Phys. **4** (1963).  
[15] A Ginzburg-Landau model for the free energy can also be used for other systems, see e.g. [21].  
[16] We only consider odd complexities in our analysis.  
[17] The notation  $S_n$  indicates the 2D block-averaged spin configuration after  $n$  time steps.  
[18] In future work, we will carry out an error analysis when only a small number of test samples is available [6, 7].  
[19]  $T_c$  refers to the critical temperature for a second order phase transition following Onsager’s [22] solution.  
[20] K. J. Gaffney *et al.*, Phys. Rev. Lett **95**, 125701 (2005).  
[21] M. E. Gracheva, J. M. Rickman, and J. D. Gunton, J. Chem. Phys. **113**, 9 (2000).  
[22] L. Onsager, Phys. Rev. **65**, 117 (1944).